Estimation of the free-charge-carrier concentration in fast-ion conducting Na_2S-B_2S_3 glasses from an analysis of the frequency-dependent conductivity

Ernest F. Hairetdinov and Nikolai F. Uvarov
Institute for Solid State Chemistry, Russian Academy of Sciences, 630091 Novosibirsk, Russia

Hitendra K. Patel and Steve W. Martin
Department of Materials Science and Engineering, Iowa State University of Science and Technology, Ames, Iowa 50011
(Received 29 June 1994)

ac and dc conductivities of fast-ion conducting $x\mathrm{Na_2S}+(1-x)\mathrm{B_2S_3}$ glasses in the composition range $0.001 \le x \le 0.1$ were analyzed using the Almond-West formula $\sigma(\nu)=\sigma_{dc}[1+(\nu/\nu_H)^{\alpha}]$. The hopping frequency for free charge carriers ν_H, the dc conductivity σ_{dc}, and their respective activation energies were determined. The concentration of free charge carriers evaluated from the conductivities and estimated mobilities is in good agreement with the overall content of sodium cations in the glasses and it is proposed that this supports the concept of a strong and not weak electrolyte model for these fast-ion conducting glasses.

I. INTRODUCTION

Recently, Almond and West[1-3] have proposed the following empirical formula to describe the frequency-dependent bulk dc/ac conductivity in ionic crystals and glasses:

$$\sigma(\nu)=\sigma_{dc}\left[1+\left[\frac{\nu}{\nu_H}\right]^{\alpha}\right], \tag{1}$$

where σ_{dc} is the low-frequency limit of the bulk conductivity, ν is the applied electrical field frequency, ν_H is the hopping frequency of charge carriers, and α is a dimensionless parameter in the range $0 \le \alpha \le 1$. The above expression predicts a power-law dependence to the conductivity for $\nu > \nu_H$.

Hairetdinov[4] suggested that this phenomenological expression may be explained by assuming that when the external field frequency ν is greater than the hopping frequency ν_H, then the free charge carriers may behave as dipoles with non-Debye-like absorption ($\alpha > 0$), characteristic of the "universal dielectric response."[5] However, this raises the question of whether it is appropriate to identify ν_H with the ion-hopping frequency. There has been both criticisms[6-8] and support[4,9-17] of this suggestion. The truth, however, of any hypothesis is shown through careful experiments designed to test its validity. As far as we know, to date no systematic experimental study of the Almond-West formula has been carried out.

To test this hypothesis, we ask the question: What is the most accurate way to experimentally check the validity of Eq. (1)? One way would be to use Eq. (1) to estimate the mobilities of free charge carriers in alkali-halide crystals combined with a conventional study of the conductivity in the intrinsic region. In accord with the Koch-Wagner treatment[18] for these systems, it is possible to estimate the concentrations, hence the mobilities, of free charge carriers in these crystals and compare them with those calculated from Eq. (1). The conductivities of alkali-halide crystals, however, are very low[18] making it difficult to measure accurately σ_{dc} and σ_{ac} for these crystals.

Another approach would be the systematic study of the possible correlation between ν_H, σ_{dc}, and the concentration of the free charge carriers in ion-conducting glasses containing varying amounts (over a few orders of magnitude) of cation conductors. Two of us have performed a very restrictive treatment of this kind[9] for three concentrations of sodium ions in silica glasses and the following relationship was found:

$$\frac{\nu_H}{\sigma_{dc}} \approx \frac{10^{11}}{c}\ \mathrm{Hz\,\Omega\,cm}, \tag{2}$$

where c is the mole fraction of the alkali oxide in the silica glass. Namikawa's relationship,[19]

$$\sigma_{dc} \approx (10^{-11}[\mathrm{Hz\,\Omega\,cm}]^{-1}) \times \nu_d, \tag{3}$$

where ν_d is the frequency of the maximum in the imaginary part of the dielectric constant [$\mathrm{Im}(\epsilon^*)$] seems to be a particular case of Eq. (2) for high alkali glasses ($c \approx 1$) studied by Namikawa.

Recently Patel and Martin[20,21] have investigated σ_{ac} in $x\mathrm{Na}_x\mathrm{S}+(1-x)\mathrm{B_2S_3}$ glasses over a wide range of sodium concentrations, $0.001 \le x \le 0.20$. It is of interest to analyze the validity of Eq. (1) in this case since the concentration of mobile ions covers such a wide range. To our knowledge no such study has been undertaken over such a wide concentration range of glass modifier ion in any type of glasses.

II. EXPERIMENT

The details of sample preparation and ac conductivity measurements have been described elsewhere.[20,21] Conductivity data covering a wide frequency (1 Hz–10 MHz) and temperature (300–500 K) range were evaluated rom experimental impedance (Z) and phase angle (φ) values

measured on a computer-controlled Solartron-1260 impedance analyzer. Only values in the measuring range of the instrument, $|Z| \leq 10^9\ \Omega$ and/or $\varphi \geq -89°$, were used in the analyses.

As was reported previously by Patel and Martin,[20,21] the real part of the ac conductivity of the glasses under investigation is frequency dependent. Two frequency-dependent regions were found: the high-frequency dependence is related to the bulk properties of the glass and the low-frequency dependence is caused by electrode polarization effects.[22] To describe the ac conductivity data over the full frequency range, however, both of these components must be taken into account. The next three subsections show the derivation for the dc conductivity, the high-frequency conductivity dispersion in the glass, and the low-frequency dispersion due to polarization effects.

A. The bulk dc conductivity

The conductivity in the frequency-independent region is due to long-range ion motion and is defined as the dc conductivity σ_{dc}. The dc conductivity for materials with only one carrier is given by

$$\sigma_{dc}=(Ze)n\mu\ , \tag{3'}$$

where Ze is the charge of the carrier, n is the concentration of mobile carriers, and μ their mobility. The concentration of mobile ions is given by

$$\begin{aligned} n &= N_0 \exp\left[-\frac{\Delta G_c}{kT}\right] \\ &= N_0 \exp\left[\frac{\Delta S_c}{k}\right] \exp\left[-\frac{\Delta H_c}{kT}\right] \\ &= N_e \exp\left[\frac{-\Delta H_c}{kT}\right], \end{aligned} \tag{4}$$

where ΔG_c is the free energy necessary to impart a carrier population, ΔS_e is the entropy, ΔH_c is the enthalpy, k is the Boltzmann constant, T is the temperature, and N_e is the effective infinite temperature ion concentration which includes the entropy term. The mobility is related to the diffusivity (D) through the Nerst-Einstein relation,[23]

$$\begin{aligned} \mu = \frac{Ze}{kT} D &= \frac{Ze}{kT} \gamma \lambda^2 \nu_H \\ &= \frac{Ze}{kT} \gamma \lambda^2 \nu_0 \exp\left[-\frac{\Delta G_m}{kT}\right] \\ &= \frac{Ze}{kT} \gamma \lambda^2 \nu_0 \exp\left[\frac{\Delta S_m}{k}\right] \exp\left[-\frac{\Delta H_m}{kT}\right] \\ &= \frac{Ze}{kT} \gamma \lambda^2 \nu_e \exp\left[-\frac{\Delta H_m}{kT}\right], \end{aligned} \tag{5}$$

where ΔG_m is the free energy for migration, ΔS_m is the entropy, ΔH_m is the enthalpy, γ is a geometric factor for ion hopping, λ is the average jump distance between mobile ion sites, ν_H is the actual ion jump frequency, ν_0 is the jump-attempt frequency of the mobile ion (approximated by the mobile ion IR resonance frequency), and ν_e is the effective jump-attempt frequency including the entropy term. From the first law of thermodynamics under conditions of constant sample volume and temperature, the enthalpy and energy-state functions are equal. For this reason, many authors have reported ΔH in the above concentration and rate equations with ΔE and we do this here. From the above derivation, the actual ion jump frequency ν_H is given by

$$\nu_H = \nu_e \exp\left[-\frac{\Delta E_m}{kT}\right]. \tag{6}$$

Finally, substituting Eqs. (4) and (5) into Eq. (3) yields the following for σ_{dc}:

$$\sigma_{dc} = \frac{N_e (Ze)^2 \gamma \lambda^2 \nu_e}{kT} \exp\left[-\frac{\Delta E_c + \Delta E_m}{kT}\right]. \tag{7}$$

This compares well with the experimentally-obtained result which is analytically described by

$$\sigma_{dc} = \frac{\sigma_0}{T} \exp\left[-\frac{\Delta E_{act}}{kT}\right], \tag{8}$$

where σ_0 is the infinite temperature limit of the dc conductivity and ΔE_{act} is the measured activation energy for dc conduction.

Unfortunately, the above treatment does not allow separate values for the individual contribution of the creation (ΔE_c) or migration (ΔE_m) free energy terms to be determined from the measured total activation energy (ΔE_{act}). In addition, the individual parameters in the pre-exponent cannot be separated because they are lumped into the single quantity σ_0. For this reason, the controversy continues with regard to the basic conduction mechanism in glass.

Most values reported for the dc conductivity are determined from ac conductivity measurements where only the frequency-independent region is considered. Almond and West[1-3] have proposed that there is information available in the frequency-dependent region to separate the ΔE_c and ΔE_m from the measured dc activation energy. This formalism is described in the next section.

B. The bulk ac conductivity

Jonscher[5] has proposed the following empirical relationship for the imaginary part of the complex ac dielectric loss χ'':

$$\chi'' \propto \left[\frac{\omega}{\omega_p}\right]^m + \left[\frac{\omega}{\omega_p}\right]^{n-1}, \tag{9}$$

where $\omega_p = 2\pi\nu_p$ is the dielectric loss peak frequency and m and n are parameters describing the slope on the high and low sides, respectively, of the dielectric loss peak. Such a formalism accurately reproduces asymmetric dielectric loss peaks for materials and liquids that exhibit purely dielectric behavior. In these cases, m is typically

close to unity and n is typically small, ~ 0.5.

For materials that exhibit a nonzero dc conductivity and do not have clearly recognizable reorientable dipoles, the imaginary part of the dielectric constant *does not* exhibit dielectric loss peaks, but rather conductivity relaxation peaks that Macedo, Moynihan, and Bose[24] have shown can be seen in the inverse of the dielectric constant, $M^*=1/\epsilon^*$, the electric modulus. Nonetheless, Eq. (1) can still be used to model the imaginary part of the dielectric constant, except that the m exponent changes sign and becomes $\sim -$unity. In these cases, ϵ'' decreases with increasing frequency in the low-frequency range, $\omega<\omega_p$, with slope near unity and at $\omega=\omega_p$, ϵ'' changes slope to $n-1$ and decreases less quickly.

Similarly, the dispersion in the real part of the conductivity $\sigma'(\omega)$ was empirically described by Almond and West[1-3] through the power-law equation:

$$\sigma'(\omega)=\sigma_{\rm dc}+A\omega^{\alpha} . \tag{10}$$

They related the real part of the complex conductivity to the dielectric loss through the following relationship:

$$\sigma'(\omega)=\omega\chi''(\omega) . \tag{11}$$

Substituting Eq. (9) into Eq. (11) they obtained the following relationship for the conductivity:

$$\sigma'(\omega)\propto\omega\left[\left[\frac{\omega}{\omega_p}\right]^{m}+\left[\frac{\omega}{\omega_p}\right]^{n-1}\right] , \tag{12}$$

and by assuming a single proportionality constant K in both the conductivity and the dielectric loss, equating the dielectric loss frequency ω_p to the ion hopping frequency, $\omega_H=2\pi\nu_H$, and letting $m=-1$ and $n=\alpha$ they obtained the following result for the ac conductivity:

$$\begin{aligned}\sigma'(\omega)&=K\omega\left[\left[\frac{\omega}{\omega_H}\right]^{-1}+\left[\frac{\omega}{\omega_H}\right]^{\alpha-1}\right]\\&=K\omega_H+K\omega_H^{1-\alpha}\omega^{\alpha} .\end{aligned} \tag{13}$$

By comparing the above equation and Eq. (10), they observed that the dc conductivity may be described by the ion-hopping frequency:

$$\sigma_{\rm dc}=K\omega_H . \tag{14}$$

Comparison of the above equation to Eqs. (6) and (7) shows that K is composed of the carrier concentration, the ion jump distance, the geometric term, the Coulomb charge, and the Boltzmann constant. Furthermore, the ac and dc conductivity terms in Eq. (10) may be related to each other through Eqs. (13) and (14) in terms of A by

$$\sigma_{\rm dc}=A\omega_H^{\alpha} . \tag{15}$$

After simplifying Eq. (13) and writing it in terms of $\sigma_{\rm dc}$, the ac conductivity may be written in a similar form as Eq. (1):

$$\begin{aligned}\sigma'(\omega)&=\sigma_{\rm dc}+\sigma_{\rm dc}\left[\frac{\omega}{\omega_H}\right]^{\alpha}\\&=\sigma_{\rm dc}\left[1+\left[\frac{\omega}{\omega_H}\right]^{\alpha}\right]\end{aligned} \tag{16a}$$

and in terms of ν:

$$\sigma'(\nu)=\sigma_{\rm dc}\left[1+\left[\frac{\nu}{\nu_H}\right]^{\alpha}\right] . \tag{16b}$$

The hopping frequency ν_H is obtained from ac conductivity when

$$\sigma'(\nu_H)=2\sigma_{\rm dc} . \tag{17}$$

Finally, substituting Eqs. (6) and (7) into Eq. (16b), the bulk ac conductivity is written in terms of physical parameters:

$$\begin{aligned}\sigma'(\nu)=&\frac{N(Ze)^2\gamma\lambda^2\nu_e}{kT}\exp\left[-\frac{\Delta E_c+\Delta E_m}{kT}\right]\\&\times\left[1+\left[\frac{\nu}{\nu_e\exp\left[-\frac{\Delta E_m}{kT}\right]}\right]^{\alpha}\right] .\end{aligned} \tag{18}$$

From Eq. (18) it is seen that the activation energies for ν_H, $\sigma_{\rm dc}$, and A are ΔE_c, $\Delta E_c+\Delta E_m$, and $\Delta E_c+(1-\alpha)\Delta E_m$, respectively. If the experimentally-determined activation energies for $\sigma_{\rm dc}$ and ν_H are the same then it implies that $\Delta E_c\approx 0$, hence the charge-carrier concentration is temperature independent and all the ions are in essence mobile and support the strong electrolyte model. If the activation energies are different, then the concentration of charge carriers is thermally activated and this would support the weak electrolyte description of these glasses.

In our calculations, the ion jump distance, λ, in the $Na_2S+B_2S_3$ glasses was assumed to be constant and approximated to Pauling's diameter of S^{2-}, 3.64×10^{-8} cm. $\gamma=\frac{1}{6}$ is the geometrical factor used for isotropic materials as is the case of glasses. We have previously analyzed the electrical modulus data for these glasses using a variable cation-cation separation distance.[20,21] In the low alkali glasses, the separation distance increases to nearly 40 Å for $x=0.001$. Although the cations may exhibit such a separation distance, it is unreasonable to assume that the cations jump this distance during a hop and as such we have differentiated between the separation distance and the jump distance in these low alkali glasses. Indeed

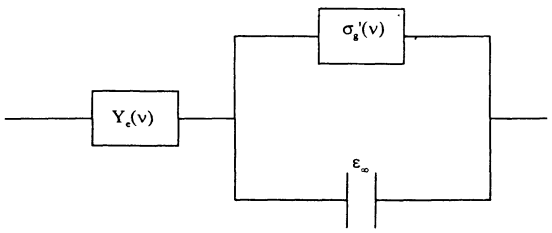

FIG. 1. Equivalent electrical circuit used for simulation of conductivity of the glasses where Y_e is the electrode admittance, σ_g' is the real part of the bulk conductivity of the sample, and ϵ_∞ is the high-frequency limit of the dielectric constant.

we have already proposed a mechanism for such a differentiation.[20]

III. ELECTRODE IMPEDANCE AND THE ac CONDUCTIVITY

To describe the total $\sigma(\nu,T)$ dependence it is necessary to determine the appropriate expression for electrode impedance. Since blocking gold electrodes were used,[20,21] the electrode impedance can be modeled in terms of either a capacitor or a complex phase admittance[22] (CPA) in series with the bulk conductivity of the glass as shown in Fig. 1. A capacitor will exhibit an ac conductivity $\sigma_{ac} \propto \nu$ as $\nu \rightarrow 0$, however, the experimental slope $d(\log_{10}\sigma)/d(\log_{10}\nu)$ appears to be less than unity. Therefore, the experimentally-measured electrode admittance may be better described by the CPA element:

$$Y^*_{CPA} = Y_e \nu^a [\cos(a) + i \sin(a)] , \tag{19}$$

where Y_e and a are parameters and $i = \sqrt{-1}$. The bulk complex conductivity for the glass, σ^*_g, modeled in Fig. (1) is given by

$$\sigma^*_g(\nu) = \sigma'_g(\nu) + i 2\pi\nu\epsilon_\infty , \tag{20}$$

where σ'_g is the real part of the glass ac conductivity defined by Eq. (18) and ϵ_∞ is the limiting high-frequency dielectric permittivity of the glass. The total complex ac conductivity, σ^*, for the glass and the electrode is determined using the following equation:

TABLE I. Values for parameters to describe the low- and high-frequency conductivity dispersion and dc conductivity were determined by fitting each conductivity isotherm to Eq. (22).

x	T (°C)	$\log_{10}(\nu_H)$ (Hz)	α	$\log_{10}(N_e)$ (cm^{-3})	$\log_{10}(Y_e)$ [$Hz^{-a}/(\Omega\,cm)$]	a
0.001	167.7	5.50	0.66	19.50	−8.6	0.71
	159.0	5.30	0.60	19.50	−8.7	0.71
	150.8	5.38	0.51	19.34	−8.8	0.78
	143.6	5.08	0.64	19.48	−8.8	0.74
	132.4	4.95	0.66	19.40		
	121.3	4.53	0.77	19.52		
	112.2	4.30	0.84	19.40		
	102.9	4.10	0.89	19.40		
0.01	152.6	5.16	0.74	20.56	−8.52	0.82
	133.1	4.71	0.72	20.59	−8.65	0.90
	123.6	4.49	0.72	20.60	−8.69	0.92
	113.8	4.25	0.72	20.60	−8.73	0.94
	94.5	3.76	0.73	20.59	−9.00	1.10
	75.2	3.27	0.76	20.54		
	54.8	2.84	0.81	20.40		
	30.0	2.28	0.81	20.32		
0.1	143.5	6.27	0.49	21.59	−9.50	0.89
	133.6	5.90	0.44	21.70	−9.52	0.89
	115.1	5.42	0.38	21.96	−9.52	0.90
	96.0	5.06	0.37	22.03	−9.51	0.90
	76.7	5.01	0.40	21.83	−9.44	0.90
	57.6	4.83	0.43	21.68	−9.45	0.90
	48.4	4.61	0.43	21.69	−9.45	0.90
	31.7	4.23	0.46	21.66	−9.45	0.90

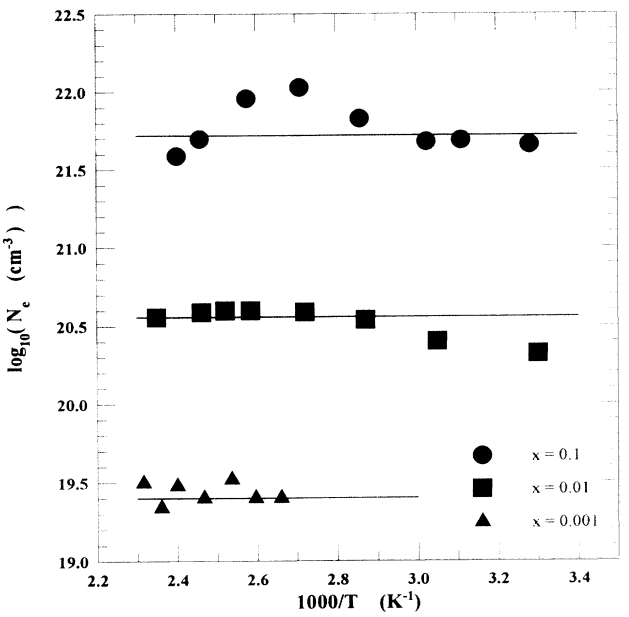

FIG. 2. The temperature dependence of $\log_{10}(N_e)$ for glass compositions $x = 0.1$, 0.01, and 0.001. The points are determined by fitting each conductivity isotherm independently to Eq. (22) and the lines are determined by fitting all the conductivity isotherms simultaneously for each glass.

$$\sigma^*(\nu) = \frac{Y^*_{CPA}(\nu) \times \sigma^*_g(\nu)}{Y^*_{CPA}(\nu) + \sigma^*_g(\nu)} . \tag{21}$$

The real part of the conductivity for the scheme presented in Fig. 1 is determined by separating the real and imaginary parts of the complex conductivity in Eq. (21) and is given below:

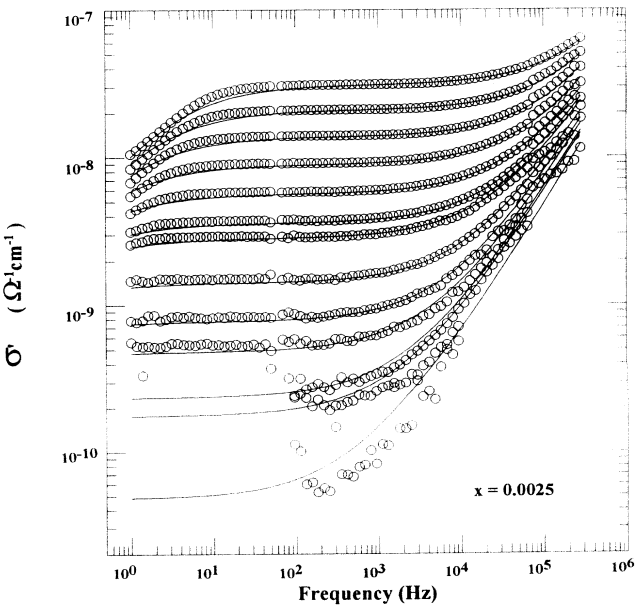

FIG. 3. Results of the fitting conductivity isotherms simultaneously to Eq. (22) for the low-alkali glass, $x = 0.0025$. The fit parameters are found in Table II.

$$\sigma'_T(\nu,T)=\frac{Y_e\nu^a[\sigma'_g Y_e\nu^a+\sigma'^2_g\cos(a)+(2\pi\nu\epsilon_\infty)^2\cos(a)]}{\sigma'^2_g+2Y_e\nu^a[\sigma'_g\cos(a)+2\pi\nu\epsilon_\infty\sin(a)]+(Y_e\nu^a)^2+(2\pi\nu\epsilon_\infty)^2}\ . \tag{22}$$

We realize that this procedure will only give an approximate description of the electrode impedance. However, the aim of this work is to extract from the complex impedance data accurate values for σ_{dc}, n_H, and hence N for the glass and to not investigate the electrode effects in detail.

IV. RESULTS AND DISCUSSION

The first question of interest is whether the parameters N and α in Eq. (18) are temperature dependent. To answer this question, each conductivity isotherm for three glass samples ($x=0.001$. 0.01, and 0.1) was independently least-squares fit to Eq. (22) to determine values for ν_H, α, N_e, Y_e, and a.

The results of these analyses are given in Table I. An Arrhenius plot of the estimated charge-carrier concentration N_e is shown in Fig. 2. Within experimental accuracy, the concentration of the free charge carriers is temperature independent, i.e., the activation energy for formation of free charge carriers is negligibly small. The slope of the conductivity dispersion α appears to be weakly temperature dependent. This may be a result of a decreasing amount of frequency-dependent conductivity data available to perform least-squares fitting as a function of temperature increase. Some increase in the value for the slope α may also be attributed to the universal dielectric response ($\alpha=0.95\pm0.05$) after Jonscher.[5]

The apparently weak temperature dependence (if any) of the parameters N_e and α make it possible to perform a second fitting of the data. In this case, all the conductivity isotherms for each glass composition were fitted simultaneously to Eq. (22) with fitting parameters being ν_H, ΔE_{act}, α, N, Y_e, and a. The result of this fitting routine for a low-alkali glass where $x=0.0025$ is demonstrated in Fig. 3 and for a "high-alkali" glass where $x=0.10$ in Fig. 4. As expected, higher alkali content glasses with their higher conductivity at equivalent temperature show much greater electrode polarization behavior, even at lower temperatures.

The solid line in Fig. 2 corresponds to the value of N_e determined using the second fitting method and the symbols represent the values determined using the first fitting method. Analyses of the remaining glasses were performed using the second fitting routine due to the good agreement between the first and second fitting methods. The results of these fittings and values for the conductivity prefactor σ_0 and σ_{dc} at $T=150$°C for all glasses are given in Table II.

The main point of this paper is presented in Fig. 5, where the log of the calculated N_e is plotted versus the log of the experimental concentration x. The solid line corresponds to N_e calculated assuming complete disassociation of the modifer Na_2S. The result here would indicate that all cations are available for conduction and would suggest a strong electrolyte picture for these glasses. The charge-carrier concentrations determined from least-squares fit, however, are systematically almost

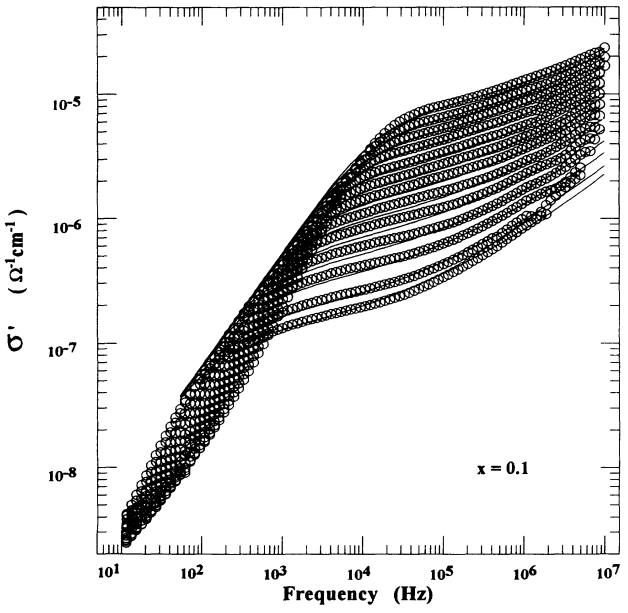

FIG. 4. An example of results obtained in fitting conductivity isotherms simultaneously to Eq. (22) for the high-alkali glass, $x=0.1$. The fit parameters are found in Table II.

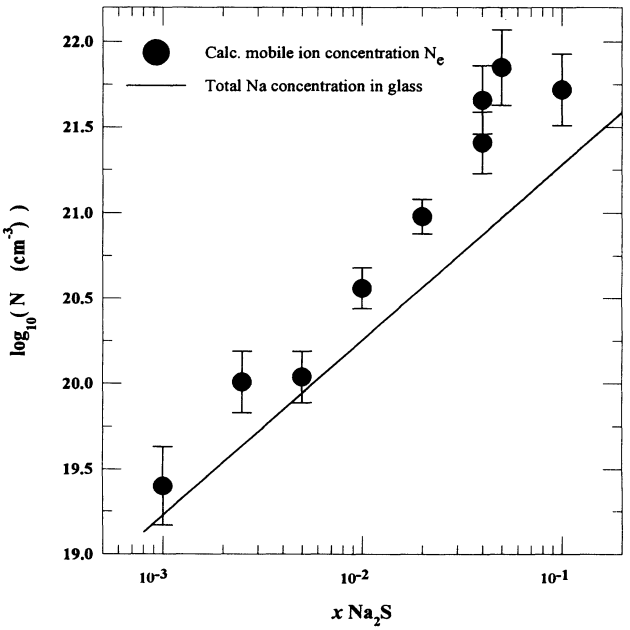

FIG. 5. Calculated concentration of the free charge carriers vs total content sodium cations. The line is the total concentration of sodium in the glass.

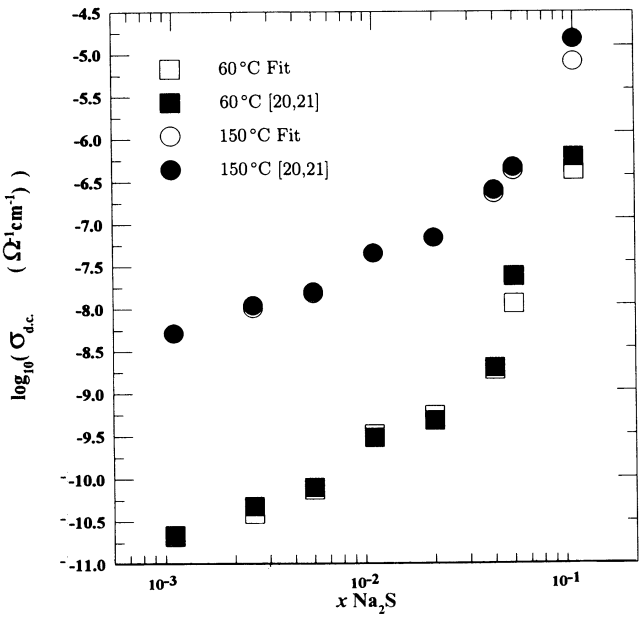

FIG. 6. Calculated (open symbols) and experimental (filled symbols) of $\log_{10}(\sigma_{dc})$ vs $\log_{10}(x)$ isotherms for 60 and 150 °C. The results are in excellent agreement with those reported by Patel and Martin (Refs. 20 and 21).

twice the value of the experimental values. This may be due to the underestimation of the jump distance. For example, assuming that the hopping distance is $\sim\sqrt{2}$ times Pauling's value for the S^{2-} ion diameter we can obtain more agreeable results for N. The problem with adjusting this parameter is that we have no reasonable explanation for a choice of the hopping distance. The anomalous calculated value of N_e for the glass $x=0.05$ is also puzzling. The possible explanation that for some reason the actual concentration of Na_2S in the glass is much higher than

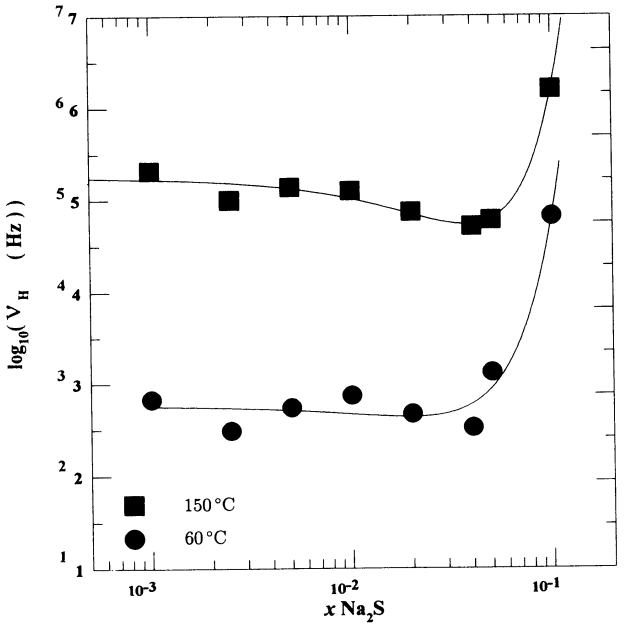

FIG. 7. Hopping frequency isotherms for 60 and 150 °C as a function of Na_2S content. The lines are only a guide for the eye.

TABLE II. Best fit values for parameters in Eqs. (18) and (22). They were determined by fitting each conductivity isotherms simultaneously to Eq. (22) for each glass composition. Calculated dc conductivity and hopping frequency values at $T=150$ °C are also reported.

x	$\log_{10}\sigma_0$ [K/(Ω cm)]	$\log_{10}\sigma_{dc}$ (150 °C) (Ω cm)$^{-1}$	$\log_{10}\nu_e$ (Hz)	ΔE_{act} (eV)	α	$\log_{10}\nu_H$ (150 °C) (Hz)	$\log_{10}N_e$ (cm^{-3})	$\log_{10}Y_e$ [Hz$^{-\alpha}$/(Ω cm)]	a
0.001	3.66±0.15	−8.28±0.11	14.63±0.23	0.78±0.03	0.60±0.22	5.32±0.23	19.4±0.23	−8.73±0.54	0.69±0.10
0.0025	3.93±0.11	−7.99±0.14	14.29±0.18	0.78±0.02	0.78±0.14	5.00±0.18	20.01±0.18	−8.36±0.44	0.70±0.11
0.005	3.91±0.12	−7.82±0.16	14.24±0.15	0.76±0.01	0.69±0.06	5.14±0.15	20.04±0.15	−8.39±0.28	0.81±0.08
0.01	3.79±0.11	−7.34±0.09	13.61±0.12	0.71±0.01	0.76±0.04	5.10±0.12	20.56±0.12	−8.57±0.21	0.84±0.08
0.02	3.95±0.09	−7.16±0.09	13.26±0.10	0.70±0.01	0.79±0.04	4.87±0.10	20.98±0.10	−8.86±0.26	0.89±0.09
0.04	3.94±0.33	−6.64±0.25	12.66±0.20	0.67±0.03	0.76±0.08	4.71±0.20	21.66±0.20	−8.43±0.19	0.77±0.07
0.04	4.08±0.17	−7.32±0.16	13.04±0.18	0.74±0.02	0.68±0.05	4.27±0.18	21.41±0.18	−8.83±0.22	0.84±0.09
0.05	2.61±0.24	−6.37±0.18	11.14±0.22	0.53±0.03	0.62±0.03	4.78±0.22	21.85±0.22	−9.21±0.37	0.85±0.24
0.1	2.67±0.25	−5.09±0.19	11.33±0.21	0.43±0.02	0.44±0.03	6.20±0.21	21.72±0.21	−9.49±0.09	0.90±0.08

the stated composition may be excluded because in Fig. 6, where conductivity isotherms are plotted vs Na_2S content, it is seen that the point corresponding to $x=0.005$ is not anomalous. The same is true for the plot of ΔE_{act} and ν_H vs $\log(x)$ shown in Fig. 7. However, the anomaly does manifest itself in the conductivity prefactor plot vs $\log(x)$ as shown in Fig. 8 and in the hopping-frequency prefactor, ν_e vs $\log(x)$ and/or the interionic Na^+-Na^+ separation distance in glasses of varying Na_2S content (Fig. 9).

It is of interest to note, in accord with the data of Fig. 6, that the conductivity increases linearly with Na_2S concentration in the range $0.001 \leq x \leq 0.05$ and suggests that the ion mobility is constant. A linear increase in conductivity with concentration is characteristic for strong electrolytes where all the alkali cations are thought to be disassociated from sulfur in these glasses. Figure 10 shows the temperature dependence of the hopping rates as determined from the first fitting method and the solid lines correspond to the second fitting method. Both the ΔE_{act} and ν_H values for $x=0.001$ and 0.01 glasses are quite similar explaining the reason for a compositionally-independent mobility in this range region.

The dramatic increase in ν_H for the $x=0.1$ glass, corresponding to the decrease in ΔE_{act} is the reason for the superlinear increase of the conductivity for $x \geq 0.05$ glasses. The lowering of activation energy barriers for ion conduction in this region is a result of increased Na^+-Na^+ ion interaction or overlap of their Coulomb energy wells due to an increase in the ion concentration (or a decrease in the ion-ion separation).[20,21] The ion concentration in this glass composition is temperature independent and therefore also behaves like a strong electrolyte.

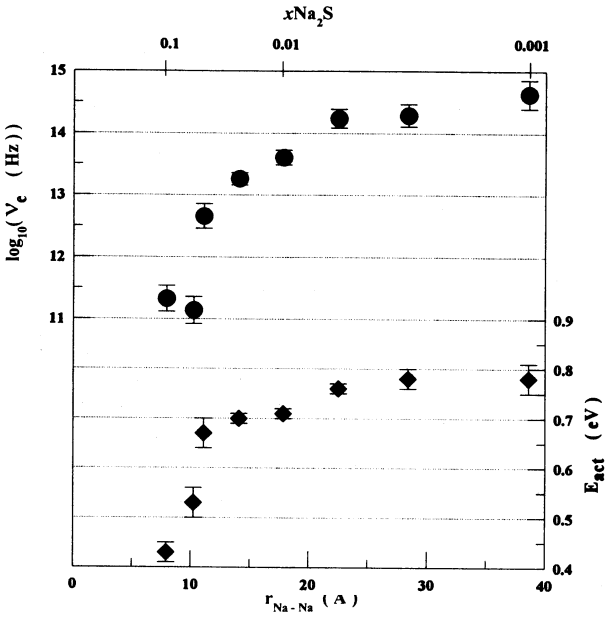

FIG. 9. Hopping rate prefactor ν_e vs Na^+-Na^+ interionic distance (bottom axis) and Na_2S content (top axis). For comparison ΔE_{act} is also plotted. The lines are only a guide for the eye.

V. CONCLUSIONS

(1) Two types of fitting procedures were used to evaluate the ionic conductivity parameters ν_e, ΔE_{act}, α, N, Y_e. and a and A in $xNa_2S+(1-x)B_2S_3$ glasses in the composition range $0.001 \leq x \leq 0.1$: (i) analysis of frequency-dependent conductivity isotherms independent of each other; (ii) analysis of experimental data for all the temper-

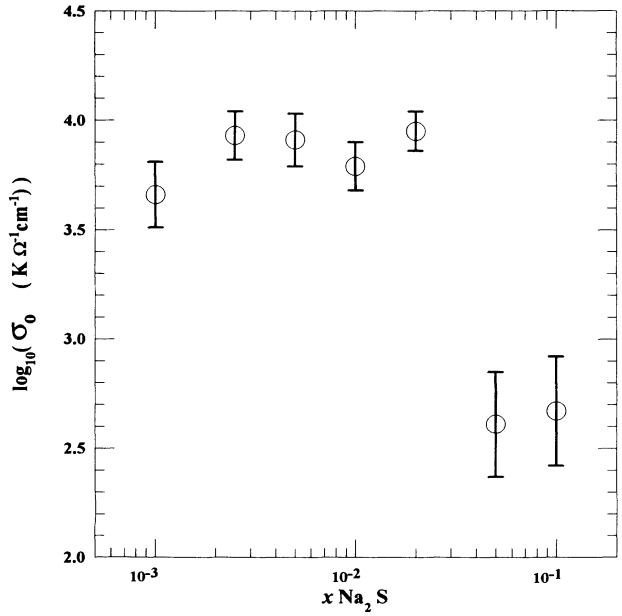

FIG. 8. Experimental prefactor σ_0 values in the expression $\sigma_{dc}T=\sigma_0\exp(-\Delta E_{act}/kT)$ as a function of Na_2S content. A sharp decrease is evident for $x=0.05$.

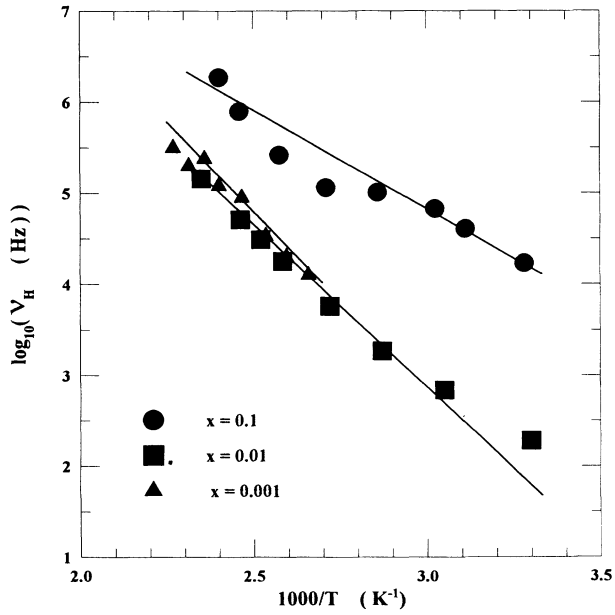

FIG. 10. The temperature dependence of the hopping rate, ν_H. The points are calculated values by fitting each isotherm and the lines are results of values determined by simultaneously fitting all the isotherms for each glass.

atures simultaneously.

(2) Estimated concentrations of free charge carriers are in reasonable agreement with overall sodium content in the glasses investigated. These glasses appear to be strong and not weak electrolytes.

(3) Conductivity for glasses in the range $0.001 \leq x \leq 0.04$ increases linearly with increase in sodium concentration lending support to the strong electrolyte concept. Superlinear increase in conductivity is observed for glasses with $x > 0.04$ and is caused by the dramatic increase in the mobility.

(4) A sharp decrease in the effective hopping rate ν_e is observed for glasses with $x\mathrm{Na_2S}$ content in the range $x \geq 0.01$. This manifests the beginning of the strong $\mathrm{Na^+}$-$\mathrm{Na^+}$ interaction in the glass matrix.

(5) The Almond-West technique does a good job in predicting the temperature and frequency dependence of experimental glass conductivity data. Microscopic parameters describing ionic conductivity in glass, namely ν_H, ν_e, ΔE_{act}, and N can also be determined using this technique.

(6) Almond and West have been criticized for developing phenomenology and not theory. The problem with developing elaborate theories, however, is that they usually cannot be tested by experiment. What Almond and West offer is a sufficiently simple method to determine basic parameters to describe temperature- and frequency-dependent ionic conductivity and it does produce testable results.

ACKNOWLEDGMENT

This work was supported by a grant from the National Science Foundation, NSF-DMR 94-04460.

[1]D. P. Almond, A. R. West, and R. Grant, Solid State Commun. **55**, 1277 (1982).

[2]D. P. Almond, A. R. West, and R. Grant, Solid State Ionics **8**, 456 (1983).

[3]D. P. Almond and A. R. West, Nature (London) **306**, 456 (1983).

[4]E. F. Hairetdinov, Izv. Sib. Otd. Akad. Nauk Ser. SSSR, Khim. Nauk **2**, 3 (1987).

[5]A. K. Jonscher, *Dielectric Relaxation in Solids* (Chelsea Dielectric, London, 1983).

[6]J. R. MacDonald and G. B. Cook, Electroanalytic. Chem. **193**, 57 (1985).

[7]H. Jain and J. N. Mundy, J. Non-Cryst. Solids **91**, 315 (1987).

[8]S. R. Elliott, Solid State Ionics **27**, 131 (1988).

[9]E. F. Hairetdinov and N. F. Uvarov, Proc. Indian Natl. Sci. Acad. **55A**, 712 (1989).

[10]N. F. Uvarov and E. F. Hairetdinov, Solid State Ionics **36**, 29 (1989).

[11]N. F. Uvarov, E. F. Hairetdinov, J. M. Reau, and P. Hagenmuller, Solid State Commun. **79**, 635 (1991).

[12]N. F. Uvarov, E. F. Hairetdinov, J. M. Reau, and P. Hagenmuller, Solid State Commun. **85**, 1025 (1993).

[13]C. T. Moynihan, J. Non-Cryst. Solids **131-133**, 1117 (1991).

[14]D. P. Almond (private communication).

[15]M. Siekierski and W. Wieczorek, Solid State Ionics **60**, 67 (1993).

[16]A. Huanosta and E. Orgaz, Solid State Ionics **62**, 69 (1993).

[17]A. Vishwanthan and S. A. Suthanthiraraj, Solid State Ionics **62**, 79 (1993).

[18]A. Lidiard, *Handbuch der Physik* (Springer-Verlag, Berlin, 1957), Vol. 20, p. 246.

[19]H. Namikawa, J. Non-Cryst. Solids **18**, 173 (1975).

[20]H. K. Patel and S. W. Martin, Phys. Rev. B **45**, 10 292 (1992).

[21]H. K. Patel and S. W. Martin, Solid State Ionics **53,-56**, 1148 (1992).

[22]P. H. Bottleberghs, in *Solid Electrolytes,* edited by P. Hagenmuller and W. van Gool (Academic, New York, 1978), p. 145.

[23]W. Kingery, H. Bowen, and D. Uhlman, *Introduction to Ceramics* (Wiley, New York, 1976).

[24]P. B. Macedo, C. T. Moynihan, and R. Bose, Phys. Chem. Glasses **13** (6), 171 (1972).